

3-phase 80 W SMPS with very wide-range input voltage based on the L6565 and ESBT[®] STC04IE170HV

1 Introduction

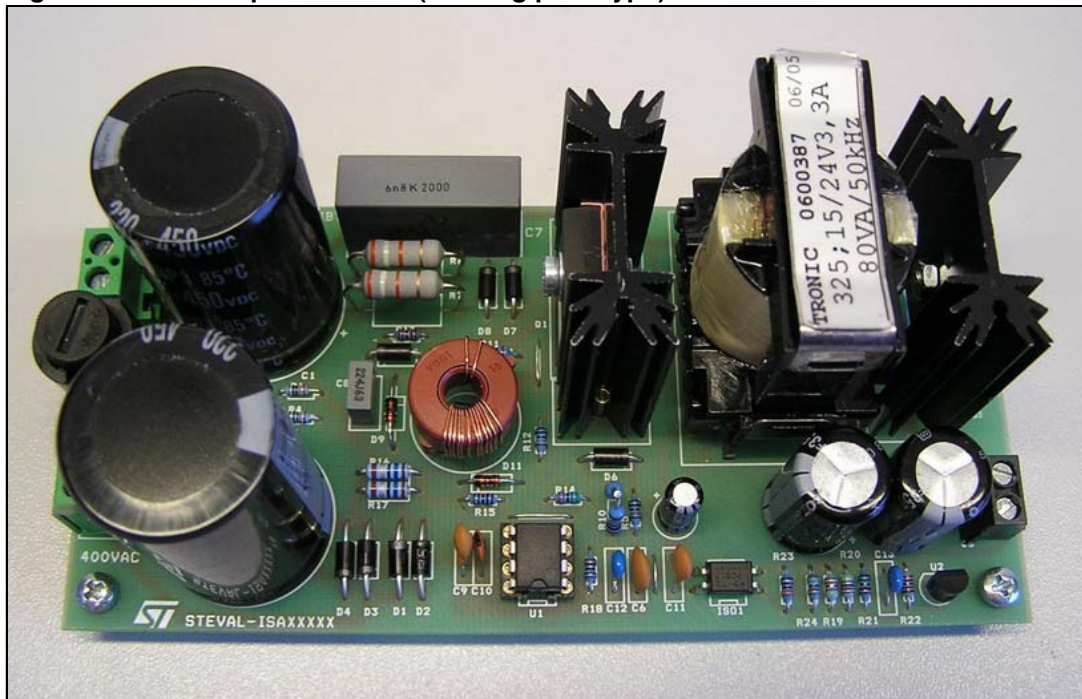
The purpose of this application note is to explain the design of an 80 W 3-phase auxiliary power supply for motor drives and welding applications. To reach a high level system in terms of both efficiency and cost, the L6565 PWM controller has been selected as well as the STC04IE170HV as the main switch. The combination of these STMicroelectronics[™] parts provides a highly efficient solution for high DC input voltage, a typical requirement of any three-phase application. The L6565 driver is a variable frequency PWM driver suitable for a design flyback converter working in quasi-resonant mode. It also includes some very useful additional features.

The frequency response study reported in this document is carried out using MATLAB.

All the design choices are thoroughly discussed to allow the user to adapt the project to specific needs. The input voltage can also be extended up to 1000 VDC as enough margin exists to do so. Finally, the experimental results are analyzed to better understand the benefits offered by the use of ESBT[®] in this application.

The document is associated with demonstration boards STEVAL-ISA019V1, STEVAL-ISA019V2 and STEVAL-ISA019V3 (*Figure 1*).

Figure 1. 80 W 3-phase SMPS (working prototype)



Contents

1	Introduction	1
2	Design specifications and L6565 brief description	5
3	Flyback stage design	6
3.1	Transformer design	8
3.1.1	Core size	8
3.1.2	Transformer losses and air gap	8
3.1.3	Wire size	10
4	Base driving circuit design	13
5	Output circuit design	16
6	Startup network design	17
7	Frequency response and loop compensation	18
8	Efficiency, waveforms and experimental results	22
9	Board modifications	26
10	References	34
11	Revision history	35

List of tables

Table 1.	Converter specification data and fixed parameters	5
Table 2.	Skin effect AC-DC resistance ratios for square-wave currents.	11
Table 3.	Transfer function main parameters	18
Table 4.	Bill of material	32
Table 5.	Document revision history	35

List of figures

Figure 1.	80 W 3-phase SMPS (working prototype)	1
Figure 2.	Flyback topology basic diagram	5
Figure 3.	Demonstration board schematic	6
Figure 4.	Dynamic magnetization curves	9
Figure 5.	Relative core losses versus frequency	10
Figure 6.	Proportional driving schematic and equivalent circuit	13
Figure 7.	Converter feedback network	19
Figure 8.	Stabilized open loop transfer function $G(s) = G_1(s) \cdot G_2(s)$ (Bode plots)	21
Figure 9.	Overall efficiency versus output power for two different values of input voltage.	22
Figure 10.	Minimum input voltage-maximum load (250 V - 80 W) in steady state	23
Figure 11.	Medium input voltage-maximum load (500 V - 80 W) in steady state	23
Figure 12.	Maximum input voltage-maximum load (850 V - 80 W) in steady state	24
Figure 13.	Very low load condition (750 V - 5 W)	24
Figure 14.	Low load condition (750 V - 24 W)	24
Figure 15.	High load condition (750 V - 80 W)	25
Figure 16.	Proportional base driving circuit relevant waveform	25
Figure 17.	STEVAL-ISA019V3	26
Figure 18.	STEVAL-ISA019V3 schematic diagram	27
Figure 19.	Power transformer EGSTON 45371	28
Figure 20.	Silk screen (top side)	29
Figure 21.	Silk screen (bottom side)	30
Figure 22.	Copper tracks	31

2 Design specifications and L6565 brief description

Table 1 lists the converter specification data and the main parameters set for the demonstration board.

Table 1. Converter specification data and fixed parameters

Symbol	Description	Values
V_{inmin}	Rectified minimum input voltage	250
V_{inmax}	Rectified maximum input voltage	850
V_{out}	Output voltage 1	24 V/3.33 A
V_{aux}	Auxiliary output voltage	15 V/0.1 A
P_{out}	Maximum output power	80 W
h	Converter efficiency	> 80%
F	Minimum switching frequency	50 kHz
V_{spike}	Max. overvoltage limited by clamping circuit	200 V

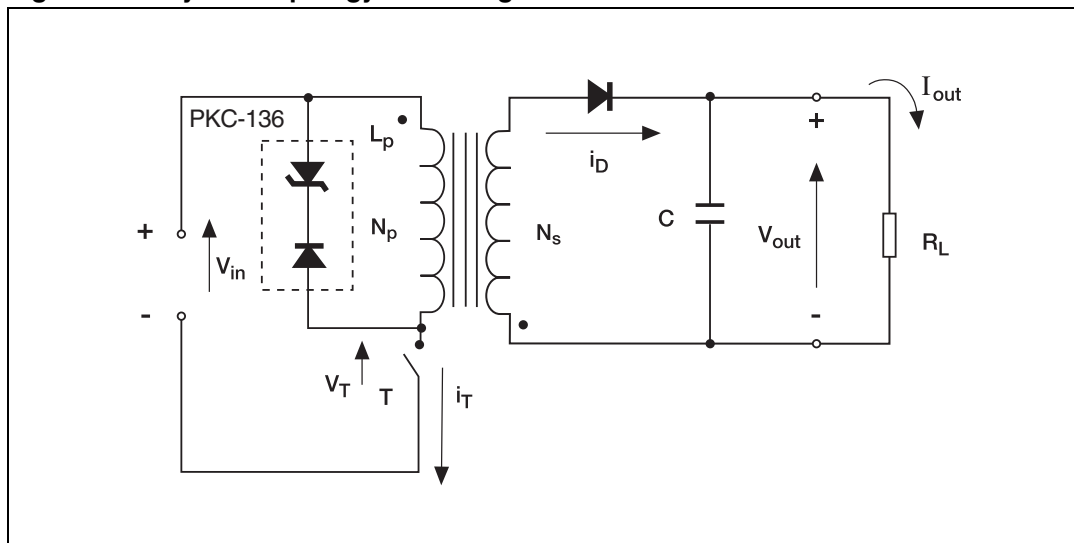
Figure 2 shows a simplified schematic diagram of a flyback converter.

The L6565 features a current mode control and is designed for flyback converters working in quasi-resonant mode and ZVS (zero voltage switching) at turn-on, or at least quasi ZVS, which means valley switching during turn-on. This condition allows the designer to reduce the power losses at turn-on as much as possible.

Since the input range is from 250 V up to 850 V, the ZVS is obtained only when $V_{in} = V_{inmin} = V_{fl} = 250$ V.

The L6565 has 8 pins. For a detailed explanation of each pin function, please refer to the L6565 datasheet.

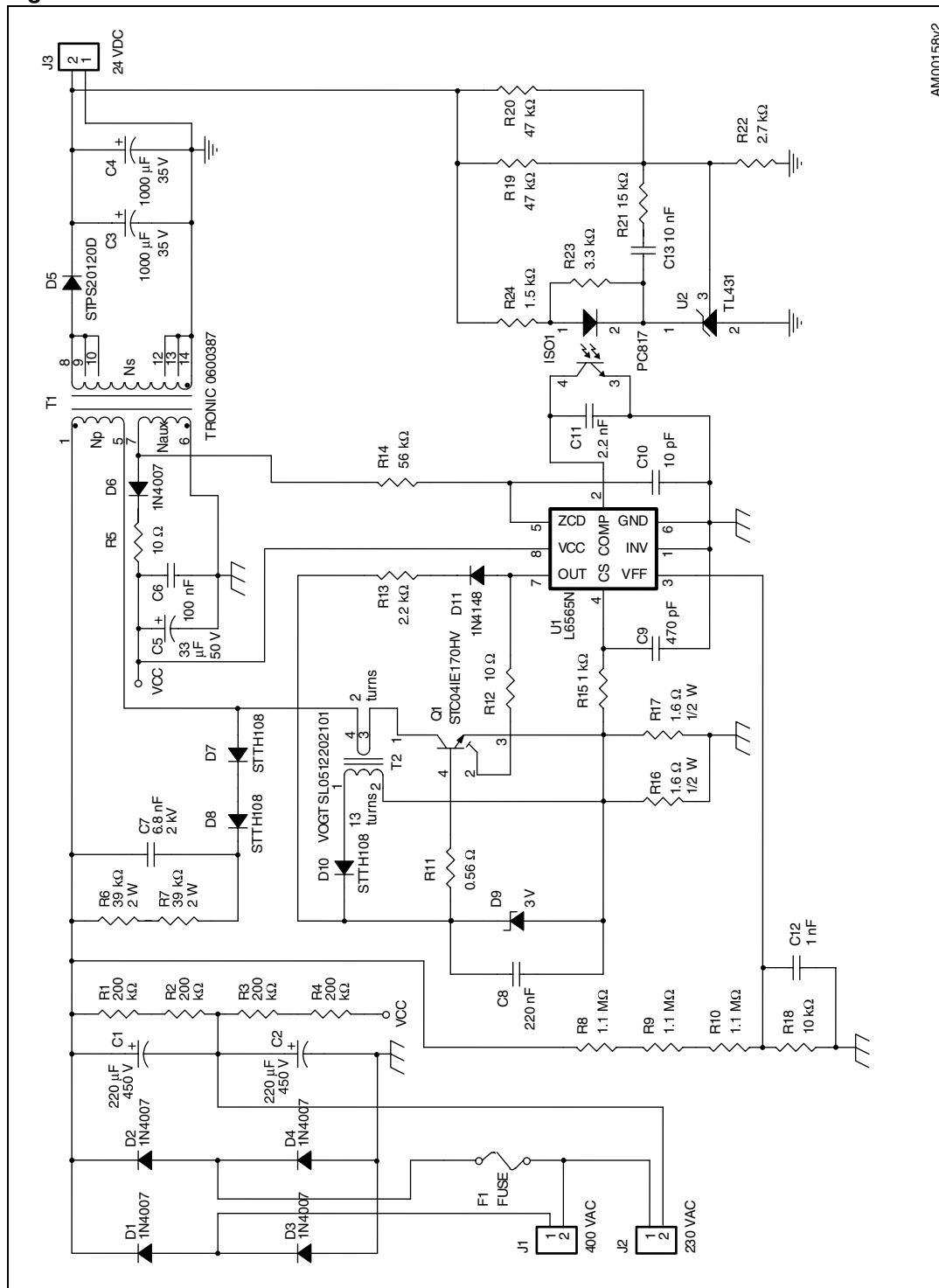
Figure 2. Flyback topology basic diagram



3 Flyback stage design

In [Figure 3](#) the complete schematic of the 80 W SMPS is shown.

Figure 3. Demonstration board schematic



AM00158v2

As commonly known, the voltage stress on the device (power switch) is given by:

Equation 1

$$V_{\text{off}} = V_{\text{inmax}} - V_{\text{fl}} - V_{\text{spike}}$$

where V_{fl} = flyback voltage = $(V_{\text{out}} + V_{\text{F, diode}}) \cdot N_{\text{p}}/N_{\text{s}}$ and V_{spike} is the maximum overvoltage allowed by the clamping network. It has been set at 200 V. N_{p} is the number of turns on the primary side, while N_{s} is the number of turns on the main output secondary winding.

Taking into account a 200 V margin, the maximum flyback voltage that can be chosen is:

Equation 2

$$V_{\text{fl}} = BV - V_{\text{inmax}} - V_{\text{spike}} - V_{\text{margin}} = 1700 - 1000 - 200 - 250 = 250\text{V}$$

After calculating the flyback voltage, proceed with the next step in the converter design.

The turn ratio between primary and secondary side is calculated with the following equation:

Equation 3

$$\frac{N_{\text{p}}}{N_{\text{s}}} = \frac{V_{\text{fl}}}{V_{\text{out}} + V_{\text{F, diode}}} = \frac{250}{24 + 1} = 10$$

As a first approximation, since the turn-on of the device occurs immediately after the energy stored on the primary side inductance has been totally transferred to the secondary side:

Equation 4

$$V_{\text{dcmmin}} T_{\text{onmax}} = V_{\text{fl}} T_{\text{reset}}$$

and

Equation 5

$$T_{\text{onmax}} + T_{\text{reset}} = T_{\text{S}}$$

where T_{onmax} is the maximum on time, T_{reset} is the time needed to demagnetize the transformer inductance and T_{S} is the switching time.

Combining the two previous equations, T_{onmax} is:

Equation 6

$$T_{\text{onmax}} = \frac{V_{\text{fl}} \cdot T_{\text{S}}}{V_{\text{dcmmin}} + V_{\text{fl}}} \cong 10\mu\text{s}$$

The next step is to calculate the peak current. According to the converter specification in [Table 1](#), output power of 80 W and desired efficiency (at least 80%), by using a formula that does not take into account the losses on the power switch, on the input bridge, and on the rectified network, we have:

Equation 7

$$P_{\text{IN}} = 1.25P_{\text{OUT}} = \frac{\frac{1}{2} \cdot L_{\text{P}} I_{\text{P}}^2}{T_{\text{S}}} = \frac{\frac{1}{2} V_{\text{dcmmin}}^2 T_{\text{onmax}}^2}{L_{\text{P}} T_{\text{S}}}$$

Hence:

Equation 8

$$L_P = \frac{V_{dcmin}^2 T_{onmax}^2}{2.5 T_S P_{OUT}} = 1.56 \text{mH}$$

Now we can calculate the peak current on primary.

Equation 9

$$I_P = \frac{V_{dcmin} T_{onmax}}{L_P} = 1.6 \text{A}$$

3.1 Transformer design

3.1.1 Core size

The core size must be chosen according to the power that must be managed, to the primary inductance, and to the saturation current as well. An approximate but efficient formula could be used as a starting point. Eventually, the designer may choose a bigger core and repeat the following steps.

Equation 10

$$A_P = 10^3 \left[\frac{L_P I_{rms(primary)}}{\Delta T^2 \cdot K_U \cdot B_{max}} \right]^{1.316} \quad [\text{cm}^4]$$

where:

- ΔT is the maximum temperature variation with respect to the ambient temperature
- K_U is the utilization factor of the window (say the portion of the window used for winding that generally ranges between 0.4 and 0.7)
- B_{max} is the maximum flux in the core.

From [Equation 10](#), we can deduct that the final best choice is an ETD34.

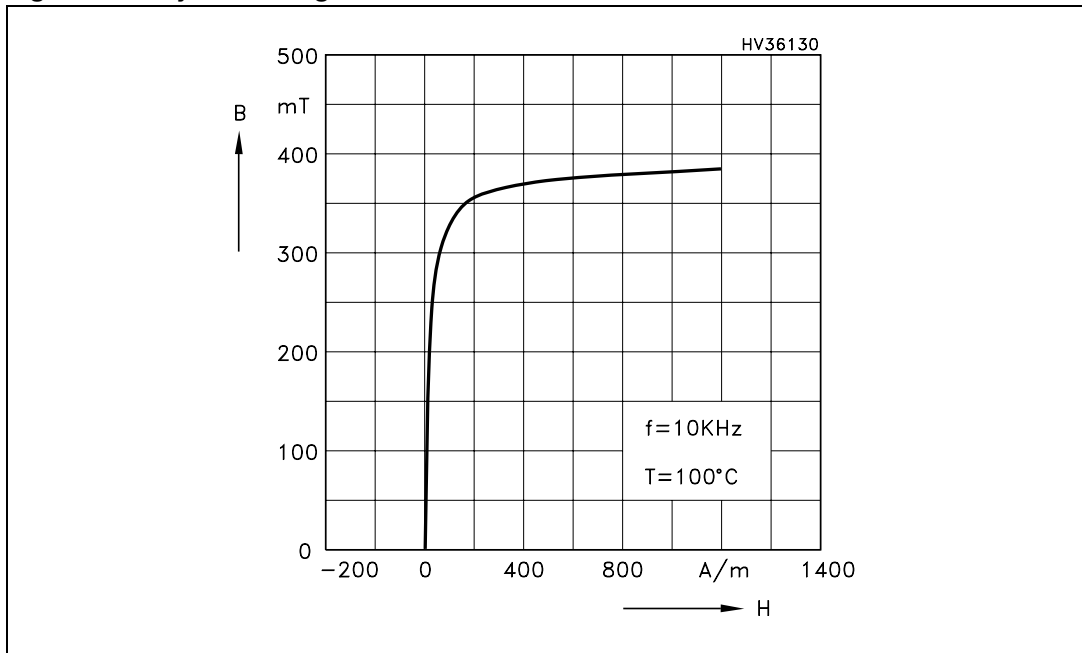
3.1.2 Transformer losses and air gap

From Faraday's law we can define the minimum primary winding turns to avoid saturation of the core. Looking at the saturation curve of the core, we can safely work up to 200 mT:

Equation 11

$$N_{pmin} = \frac{V_{in, min} \cdot T_{O(N, max)}}{\Delta B \cdot A_e} = \frac{250 \cdot 10\mu}{0.200 \cdot 97\mu} = 117$$

Figure 4. Dynamic magnetization curves



Concerning the gap, from the EPCOS datasheet, we can use the following approximate equation:

Equation 12

$$l_g = \text{gaplength} = \left(\frac{A_L}{K_1} \right)^{\frac{1}{K_2}}$$

$K_1 = 153$, $K_2 = -0.713$, while A_L has to be calculated.

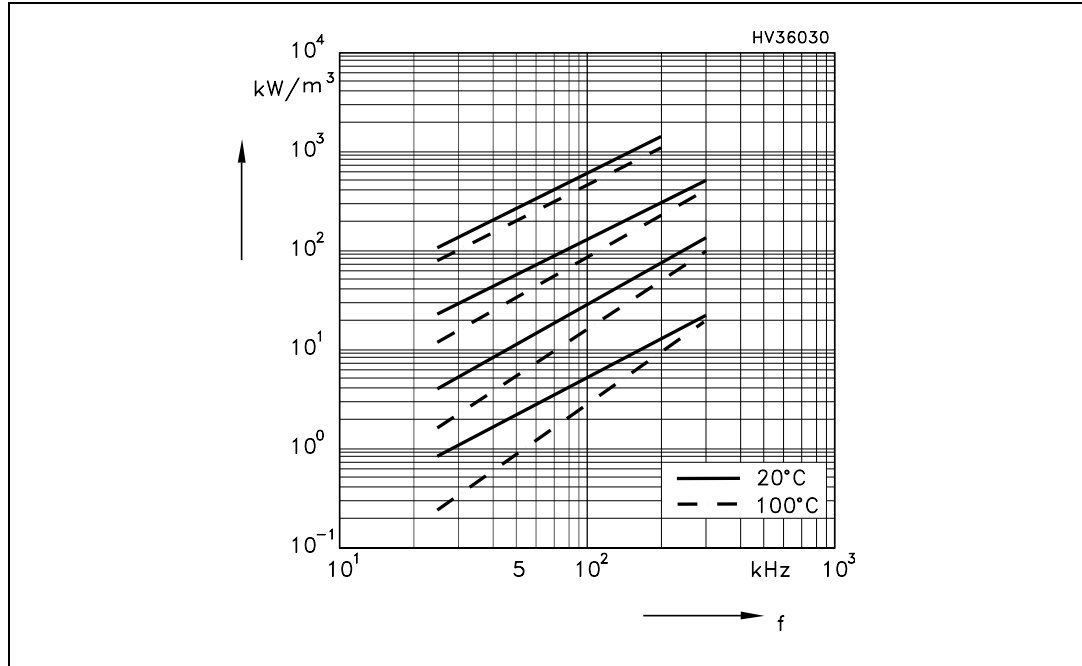
Knowing that $L_p = 1.56\text{mH}$ and $N_p = 120$,

Equation 13

$$A_L = \frac{L_p}{N_p^2} = \frac{1.56\text{m}}{120^2} = 108\text{nH}$$

$$\text{Hence: } l_g = \text{gaplength} = \left(\frac{108}{153} \right)^{-\frac{1}{0.713}} = 1.63\text{mm}$$

Figure 5. Relative core losses versus frequency



From [Figure 5](#), operating at 50 kHz with 220 mT flux excursion, the power dissipation density is about 300 mW/cm³. Once again, referring to the EPCOS datasheet, the total volume of ETD 34 is 7.63 cm³, therefore:

Equation 14

$$P_{core} = 0.3 \cdot 7.6 = 2.29W$$

Assuming a 95% efficiency for the transformer, only 4 W can be lost on it, of which about 2.3 is lost on the core while the residual 1.7 W is dissipated on the copper. Achieving this efficiency is detailed in the following [Section 3.1.3: Wire size](#).

3.1.3 Wire size

To chose the right wire size we must know the rms current on both the primary and secondary sides. Since $I_{peak, primary} = 1.6 A$ and $I_{peak, secondary} = 16 A$

Equation 15

$$I_{rms, primary} = 0.65A \quad \text{and} \quad I_{rms, secondary} = 6.53A$$

By imposing a 1 W loss on the primary side wire, the maximum series resistance can be calculated as follows:

From Joule’s law we can calculate the resistance of both the primary and secondary windings.

Equation 16

$$R_P = \frac{P_{CU, pri}}{I_{PRMS}^2} \Rightarrow R_P = 2.36\Omega \quad R_S = \frac{P_{CU, sec}}{I_{SRMS}^2} \Rightarrow R_S = 0.016\Omega$$

From that, knowing the copper resistivity at 100 °C ($\rho_{100} = 2.303 \cdot 10^{-6} \Omega \text{ cm}$), and the average wind length L_t ($L_t = 5.6 \text{ cm}$), we can easily calculate the wire sections (in cm^2).

Equation 17

$$A_{\text{PCU}} = \frac{\rho_{100} N_p L_t}{R_p} = 6.54 \cdot 10^{-4} \quad [\text{cm}^2] \Rightarrow d_p = 0.028 [\text{cm}]$$

Equation 18

$$A_{\text{SCU}} = \frac{\rho_{100} N_s L_t}{R_s} = 0.0096 \quad [\text{cm}^2] \Rightarrow d_s = 0.011 [\text{cm}]$$

[Table 2](#) provides the skin effect resistance ratios due to Eddy currents for different frequencies.

Table 2. Skin effect AC-DC resistance ratios for square-wave currents

Wire no.	Diameter d, mils	25 kHz			50 kHz			100 kHz			200 kHz		
		Skin depth S, mils	d/S	R_{ac}/R_{dc}	Skin depth S, mils	d/S	R_{ac}/R_{dc}	Skin depth S, mils	d/S	R_{ac}/R_{dc}	Skin depth S, mils	d/S	R_{ac}/R_{dc}
12	81.6	17.9	4.56	1.45	12.7	6.43	1.55	8.97	9.10	2.55	6.34	12.87	3.50
14	64.7	17.9	3.61	1.30	12.7	5.08	1.54	8.97	7.21	2.00	6.34	10.21	2.90
16	51.3	17.9	2.87	1.10	12.7	4.04	1.25	8.97	5.72	1.70	6.34	8.09	2.30
18	40.7	17.9	2.27	1.05	12.7	3.20	1.15	8.97	4.54	1.40	6.34	6.42	1.85
20	32.3	17.9	1.80	1.00	12.7	2.54	1.05	8.97	3.60	1.25	6.34	5.09	1.54
22	25.6	17.9	1.43	1.00	12.7	2.02	1.00	8.97	2.85	1.10	6.34	4.04	1.30
24	20.3	17.9	1.13	1.00	12.7	1.60	1.00	8.97	2.26	1.04	6.34	3.20	1.15
26	16.1	17.9	0.90	1.00	12.7	1.27	1.00	8.97	1.79	1.00	6.34	2.54	1.05
28	12.7	17.9	0.71	1.00	12.7	1.00	1.00	8.97	1.42	1.00	6.34	2.00	1.00
30	10.1	17.9	0.56	1.00	12.7	0.80	1.00	8.97	1.13	1.00	6.34	1.59	1.00
32	8.1	17.9	0.45	1.00	12.7	0.84	1.00	8.97	0.90	1.00	6.34	1.28	1.00
34	6.4	17.9	0.36	1.00	12.7	0.50	1.00	8.97	0.71	1.00	6.34	1.01	1.00

Note: To completely avoid the skin effect, the maximum diameter allowed is 20.3 mils, which is equal to 0.5 mm.

For practical considerations, to better optimize the utilization of the transformer window, and comply with [Equation 15](#) to [Equation 18](#) and [Table 2](#), it can be determined that:

Equation 19

$$d_s = 0.05[\text{cm}]3\text{inparallel}$$

The specifications of the transformer according to the above calculations are listed below.

Application specifications

Safety information - IEC EN60950

- $V_{inmin} = 250 \text{ V DC}$
- $V_{inmax} = 850 \text{ V DC}$
- $P_{outmax} = 80 \text{ W}$
- $V_{out} = 24 \text{ V}$ (power output 80 W)
- $I_{outmax} = 3.33 \text{ A}$
- $V_{aux} = 15 \text{ V}$ (to drive the IC < 1 W)
- $F_{swmin} = 50 \text{ kHz}$ (max. load, min. V_{in})
- $V_{flyback} = 250 \text{ V}$
- $I_{peak(primary)} = 1.6 \text{ A}$
- $I_{rms(primary)} = 0.65 \text{ A}$
- $I_{peak(secondary)} = 16 \text{ A}$
- $I_{rms(secondary)} = 6.5 \text{ A}$
- L_p (primary inductance) = 1.56 mH
- $N_p/N_s = 10$
- $N_p/N_{aux} = 17$

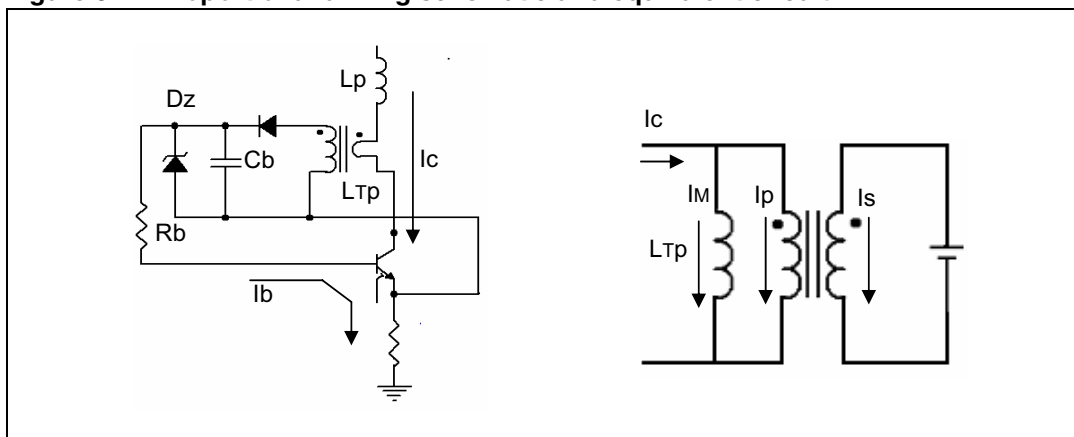
Wires and ferrite used

- $N_p = 120$ $d = 0.28 \text{ mm}$
- $N_s = 12$ $d = 0.5 \text{ mm}$ 3 in parallel
- $N_{aux} = 7$ $d = 0.28$ or smaller
- The core used is an ETD 34, N67 material from EPCOS or equivalent.
- Air gap = 1.8 mm

4 Base driving circuit design

In practical applications such as SMPS where the load is variable, the collector current is variable as well. As a consequence it is very important to provide a base current to the device which is related to the collector. In this way it is possible to avoid device over-saturation at low load and to optimize the performance in terms of power dissipation. The best and simplest way to do this is the proportional driving method provided by the current transformer in *Figure 6*. At the same time, it is very useful to provide a short pulse to the base to make the turn-on as fast as possible and to reduce the dynamic saturation phenomenon. The pulse is achieved by using the capacitor and the Zener diode in *Figure 6*.

Figure 6. Proportional driving schematic and equivalent circuit



The I_C/I_B ratio is fixed once the current transformer turn ratio has been chosen. From the ESBT STC04DE170 datasheet, and especially looking at the storage time characterization, it is clear that a turn ratio equal to 5 is a good value to ensure the right saturation of the ESBT at $I_C = 2\text{ A}$, so that in the current transformer we can first fix:

Equation 20

$$\frac{N_P}{N_S} = \frac{1}{5}$$

The core magnetic permeability of current transformer must be as high as possible to minimize the magnetization current I_M (which is not transferred to the secondary side but only drives the core into saturation). On the contrary, a too high permeability core may lead the core into saturation even with a very small magnetization current. To avoid saturation, it is necessary to increase the number of primary turns and the size of the core as well. If a core with a very small magnetic permeability is chosen, it is possible to reduce the number of primary turns and the core size. If the permeability is too small, we may not have current on the secondary side because almost all the collector current becomes magnetization current. As a compromise, a ferrite material with a relative permeability in the range 4500-7000 is the best choice.

After selecting the ferrite ring diameter, the minimum primary turns is determined to avoid core saturation from the preliminarily fixed turn ratio N with 0.2. By applying Faraday's law and imposing the maximum flux B_{\max} equal to $B_{\text{sat}}/2$:

Equation 21

$$V_1 = N_{\text{TP}} \cdot \frac{d\phi}{dt} \cong N_{\text{TP}} \cdot A_e \cdot \frac{\Delta B}{\Delta T} \Rightarrow N_{\text{TP}} = 2 \cdot \frac{V_1 \cdot T_{\text{onmax}}}{A_e \cdot B_{\text{sat}}}$$

where B_{sat} is the saturation flux of the core which depends on the magnetic permeability.

During the conduction time, the junction base-emitter of the ESBT can be seen as a forward-biased diode. To complete the secondary side load loop, the voltage drop on both diode D and resistor R_B must be added in series with the base of the ESBT. The equivalent secondary side voltage source is given by:

Equation 22

$$V_S = V_{\text{BEon}} - V_D - V_{R_B} \cong 2.5V$$

Since the magnetization inductance cannot be neglected, only I_P , a fraction of the total collector current, is transferred to the secondary. As a result, the magnetization current has to be first as low as possible. Meanwhile, the value of the magnetization inductance must be taken into account for the proper calculation of transformer primary turns and turns ratio. The magnetization voltage drop, that is, the voltage at the primary of the current transformer, can now be easily calculated:

Equation 23

$$V_1 = V_S \cdot \frac{N_{1T}}{N_{2T}} = 2.5 \cdot \frac{1}{5} = 0.5(V)$$

The magnetization current will be:

Equation 24

$$I_{\text{Mmax}} = \frac{V_1 T_{\text{ONmax}}}{L_{\text{TP}}}$$

The number of primary turns should be increased if I_{Mmax} is relatively high. The core must have a window area large enough to hold all primary and secondary windings. Otherwise it is necessary to choose a bigger core size. Once both core material and size are fixed, the turn ratio must be adjusted to get the desired I_C/I_B ratio according to [Equation 25](#) below:

Equation 25

$$N_{\text{eff}} = \frac{I_P}{I_B} = \frac{I_{\text{Cmax}} - I_{\text{Mmax}}}{\frac{I_C}{5}}$$

where I_{Mmax} is the maximum magnetization current.

The insulation between primary and secondary should be considered since the voltage on the primary side during the off time can surpass 1500 V.

The next step is to select the Zener diode, the capacitor C_b , and the resistor R_b . The turn-on performance of the ESBT is related to the initial base peak current and its duration t_{peak} , which is given approximately by [Equation 26](#):

Equation 26

$$t_{peak} = 3R_b C_b$$

A suitable value for R_b is 0.56Ω . It can eliminate the ringing on the base current after the peak, and at the same time, it generates negligible power dissipation.

The value t_{peak} can be determined once the minimum ON time is set based on the operating frequency. Bear in mind that in practical applications, it should never be lower than 200 ns. The value of C_b can be counted since the values of t_{peak} and R_b are known.

I_{peak} must be limited to avoid extra saturation of the device. The Zener diode D_z controls this and clamps the voltage across the small capacitor C_b . The Zener diode must be chosen according to the following empirical formulas and inside the range of V_{Zmin} and V_{Zmax} :

Equation 27

$$V_{Zmax} = 2(I_{peak}R_b + 1) \quad V_{Zmin} = 2(I_{peak}R_b)$$

The base peak current is higher with higher clamp voltage (D_z) or smaller capacitance (C_b), which in turn will lead to shorter duration of the peak time.

The higher and longer the base peak current is, the lower the power dissipation during turn-on. The designer must limit the I_b peak both in terms of amplitude and time duration. Otherwise, at low load a very high saturation level may result. If the device is oversaturated, the storage time is too long with higher power dissipation during turn-off. Moreover, a long storage time can also lead to output oscillation, especially at high input voltage. To overcome these problems, it is recommended to set the peak duration to 1/3 the minimum duty cycle.

Following all the equations mentioned in this section applied to the present work gives:

Equation 28

$$N_{TP} = 2 \cdot \frac{V_1 \cdot T_{onmax}}{A_e \cdot B_{sat}} \approx 2$$

where A_e is the magnetic area, considering a ring core with 12.5 mm diameter, and the saturation field B_{sat} is 400 mT.

From the first approximated assumption NS should be 10. From bench verification it is very simple to verify that the turn ratio to get the best trade-off between conduction and turn-off losses is 6.

Of course, this verification and final decision has been taken after setting all the other components in the driving network and exactly:

Equation 29

$$t_{peak} = 3R_b C_c = 400ns = C_b = 238nF = C_b = 220nF \text{ (closest commercial value)}$$

Finally, the Zener diode has been set to 3 V.

5 Output circuit design

To choose the output capacitor, the series resistance of the electrolytic capacitor must be defined.

It is well known that the main cause of the output ripple is the series resistance of the electrolytic capacitor, known as ESR, while the capacitive ripple is absolutely negligible.

Therefore, with a known secondary side peak current of 16 A and imposing a resistive ripple equal to 2% (0.48 V), we have:

Equation 30

$$ESR < \frac{V_{\text{ripple}}}{I_{SP}} = \frac{0.48}{16} = 0.03\Omega$$

Using very low ESR output capacitances, from the catalogue we get the equation $ESR \cdot C = 32e^{-6}s$ from which:

Equation 31

$$C_{\text{out}} > \frac{32 \cdot 10^{-6}}{ESR} = 1066\mu\text{F}$$

To obtain some margin and better thermal spread, the final choice is to use two 680 μF capacitors in parallel.

From Kirchoff's voltage law we can calculate the maximum voltage stress on the output diode:

Equation 32

$$V_{\text{off-diode}} = V_{\text{out}} + \frac{N_S}{N_P} \cdot V_{\text{inmax}} = 109\text{V}$$

Finally, adding a 10% margin, the STPS20120D has been selected.

6 Startup network design

To allow the circuit to start as soon as the line voltage is applied, it is necessary to pre-charge both C_5 and C_8 capacitances.

A resistor connected to the DC bus directly makes the pre-charge of C_5 electrolytic capacitance. The circuit must start at a minimum DC input voltage of 250 V. The current required by the L6565 driver during the startup time determines the $(R_1 + R_2 + R_3 + R_4)$ value. Considering that the L6565 driver needs a 0.07 mA maximum startup current, we obtain:

Equation 33

$$(R_1 + R_2 + R_3 + R_4) < \frac{V_{inmin}}{I_{SU}} = \frac{250V}{0.07mA} \cong 3.6M\Omega$$

Startup resistance must be lower than 3.6 M Ω to reach the best trade-off between power dissipation and time-to-start. As a consequence, before choosing the startup resistor, we must determine the C_5 capacitance value, which is set according to another requirement. C_5 must be able to supply the L6565 driver until the steady state behavior of the converter is established. The time from bench verification is 20 ms maximum. Given a L6565 minimum hysteresis-voltage (difference between startup threshold and undervoltage threshold) of 3.7 V, the voltage across C_5 must decrease less than 3.7 V during the startup period. From the L6565 datasheet we know that maximum quiescent current after turn-on is 3.5 mA, so C_5 must be chosen such that:

Equation 34

$$\Delta V = \frac{I_Q \cdot \Delta t}{C_5} < 3.7V \Rightarrow C_5 > \frac{3.5mA \cdot 20ms}{3.7V} \cong 19\mu F$$

$C_5 = 33 \mu F$ is a good choice to guarantee a good margin.

Finally, we can set the startup resistance value to reduce time-to-start and simultaneously optimize standby power dissipation. The L6565 has a maximum startup threshold of 14.5 V, therefore the maximum time-to-start is approximately:

Equation 35

$$\text{Time - to - start} = \frac{C_5 \cdot 14.5V}{\left(\frac{V_{inmin}}{(R_1 + R_2 + R_3 + R_4)}\right) - I_{SU}} \leq 2\text{sec} \Rightarrow (R_1 + R_2 + R_3 + R_4) \leq 808k\Omega$$

A good choice is to put in series four 200 k Ω resistors ($R_1 = R_2 = R_3 = R_4 = 200 \text{ k}\Omega$), which dissipate less than 1 W of standby power.

The pre-charge of C_8 base capacitance is carried out by connecting it to the OUT pin of the L6565 through a diode in series with a 2.2 k Ω resistor.

7 Frequency response and loop compensation

The transfer function in the complex frequency domain of the discontinuous current mode (DCM) flyback converter with L6565 driver is given by:

Equation 36

$$G_1(s) = \frac{V_{out}(s)}{V_{comp}(s)} = \frac{n \cdot R_{out} \cdot (1 - D_{max})}{2 \cdot R_S \cdot (1 + D_{max})} \cdot \frac{(1 + s \cdot C_{out} \cdot ESR) \left(1 - s \cdot \frac{L_p D_{max}}{n^2 R_{out} (1 - D_{max})^2} \right)}{1 + s \cdot \frac{C_{out} R_{out}}{1 + D_{max}}}$$

The parameters and values are listed in [Table 3](#).

Table 3. Transfer function main parameters

Parameter	Description	Value
n	Primary/secondary turn-ratio	10
R _S	Sensing resistor	0.8 Ω
D _{max}	Maximum duty-cycle	0.5
ESR	Electrolytic series resistance	16 mΩ
R _{out} = V _{out} /I _{out}	Output load	7.2 Ω
C _{out}	Output capacitance	2 mF
L _p	Primary inductance	1.56 mH

It is worth noting that the transfer function has one pole and one zero on the left half plane and an additional zero on the right half plane. The RHP zero is very difficult, if not impossible, to compensate and therefore must be kept well beyond the closed-loop bandwidth. As a result, the transient response of such a system will not be extremely fast.

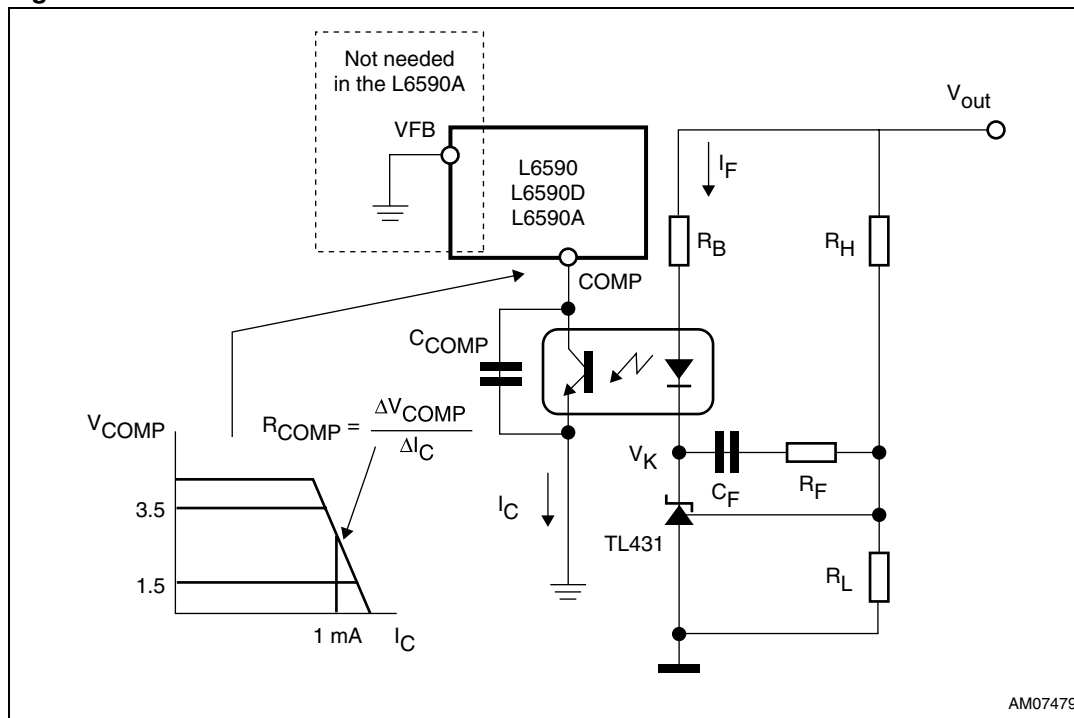
Poles and zeros are given in [Equation 37](#) and [Equation 38](#):

Equation 37

$$f_p = 25\text{Hz}; f_{z1} = 3.5 \cdot 10^5\text{Hz}; f_{z2} = 5 \cdot 10^3\text{Hz}$$

A good line and load regulation implies a high DC gain, thus the open loop gain should have a pole at the origin. Normally in this case we need a feedback network like the one in [Figure 7](#).

Figure 7. Converter feedback network



Its transfer function, which comprises a pole at the origin and a zero-pole pair, is given by:

Equation 38

$$G_2(s) = \frac{v_{comp}(s)}{V_{out}(s)} = \frac{CTR_{max} \cdot R_{COMP}}{R_B R_H C_F} \cdot \frac{1}{s} \cdot \frac{1 + s(R_H + R_F)C_F}{1 + sR_{COMP}C_{comp}}$$

The task of the control loop design is then to determine the transfer function $G_2(s)$ to ensure that the resulting closed-loop system is stable and performs well in terms of dynamic response, and line and load regulation. It is well known that the characteristics of the closed-loop system can be inferred from its open loop transfer function properties, that is $G(s) = G_1(s) \cdot G_2(s)$.

Frequency response requirements are summarized below:

1. Optimum dynamic performance requires a large gain bandwidth, that is the open loop cross-over frequency f_c to be typically chosen equal to $f_{sw}/5$ ($f_c = 10$ kHz).
2. Phase margin ϕ_m comprised between 45° and 90° is used as a design guideline. This ensures fast transient response with very little ringing. Sometimes this is not enough and so phase shift should be lower than 180° at any frequency below f_c , because a phase shift over 180° would result in a conditionally stable system.
3. Good load and line regulation implies a high DC gain (this requirement is ensured by the feedback network, whose transfer function has a pole at the origin).

First choose a typical value for $R_L = R_{22} = 2.7$ k Ω

From the L6565 datasheet we know that $I_{comp} = 5 \text{ mA}$ (source current) and $R_{comp} = 15 \text{ k}\Omega$ and can obtain:

Equation 39

$$R_B = R_{24} < \frac{V_{out} - (V_{ref} - V_{diode})}{I_{comp}} = \frac{24V - 3.5V}{5mA} = 4.1k\Omega$$

$R_{24} = 1.5 \text{ k}\Omega$ is a good choice. It is good practice to put a $3.3 \text{ k}\Omega$ resistor ($R_{23} = 3.3 \text{ k}\Omega$) in parallel to the photodiode.

The resistive partition must be set with high precision according to the following equation:

Equation 40

$$R_{high} = R_{22} \cdot \frac{V_{out} - V_{ref}}{V_{ref}} = 23.2k\Omega$$

There is no next close commercial value so it is a good idea to put two $47 \text{ k}\Omega$ resistors ($R_{19} = R_{20} = 47 \text{ k}\Omega$) in series.

Now C_{11} (C_{comp}), C_{13} (C_F) and R_{21} (R_F) must be set in order to satisfy frequency response requirements.

A good choice is to set the pole of $G_2(s)$ so as to cancel the low frequency zero of $G_1(s)$:

Equation 41

$$\frac{1}{2\pi \cdot R_{comp} \cdot C_{comp}} = 5kHz \Rightarrow C_{11} = C_{comp} \cong 2.12nF$$

The next close commercial value for $C_{11} = 2.2 \text{ nF}$ has been chosen.

Similarly C_{13} and R_{21} have been determined by setting the corresponding zero close to the pole of $G_1(s)$ and imposing the open loop gain to cross the 0 dB axis only once at $f = f_c = 10 \text{ kHz}$:

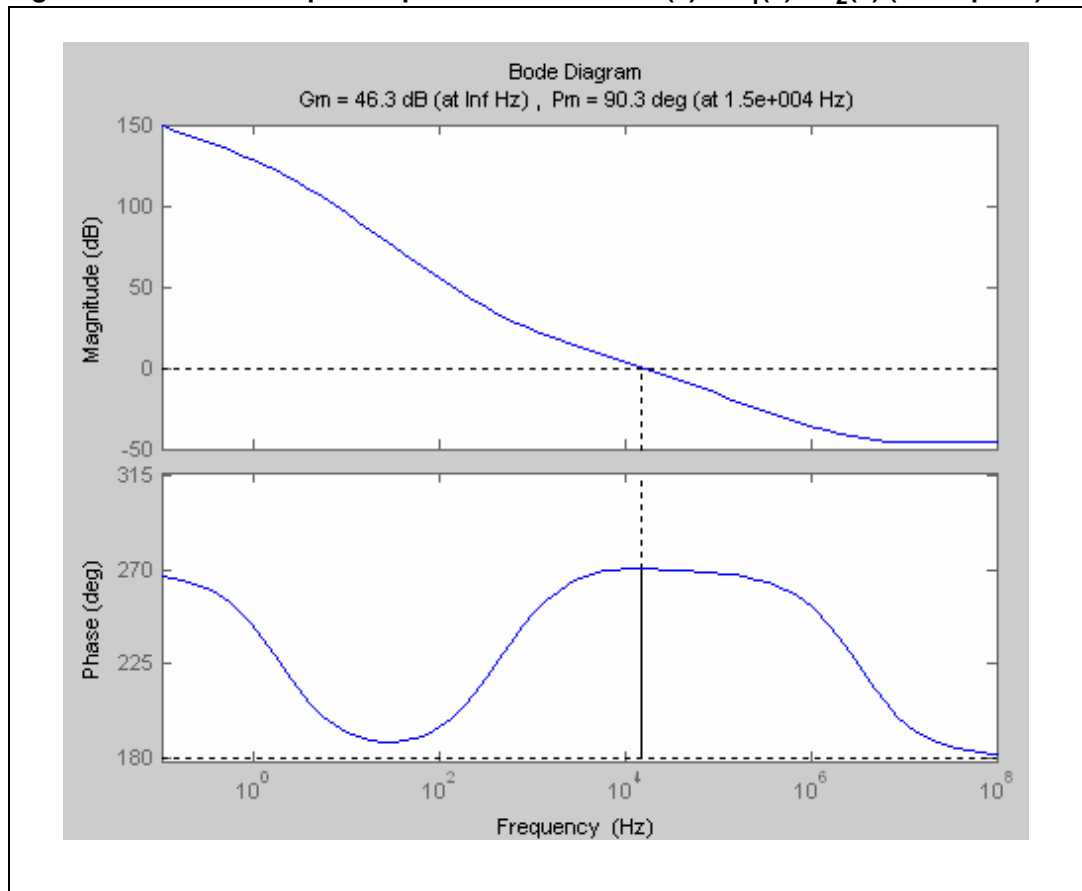
Equation 42

$$\left\{ \begin{array}{l} \frac{1}{2\pi \cdot (R_H + R_F) \cdot C_F} = 400Hz \Rightarrow C_{13} = 10nF \\ |G(j\omega)|_{\omega = 2\pi \cdot 10^4 \text{ rad/sec}} = 1 \Rightarrow R_{21} \cong 15k \end{array} \right.$$

In such a way we ideally get a phase margin of 90 degrees and an adequate closed-loop bandwidth.

Figure 8 shows Bode plots of the stabilized open loop transfer function.

Figure 8. Stabilized open loop transfer function $G(s) = G_1(s) \cdot G_2(s)$ (Bode plots)

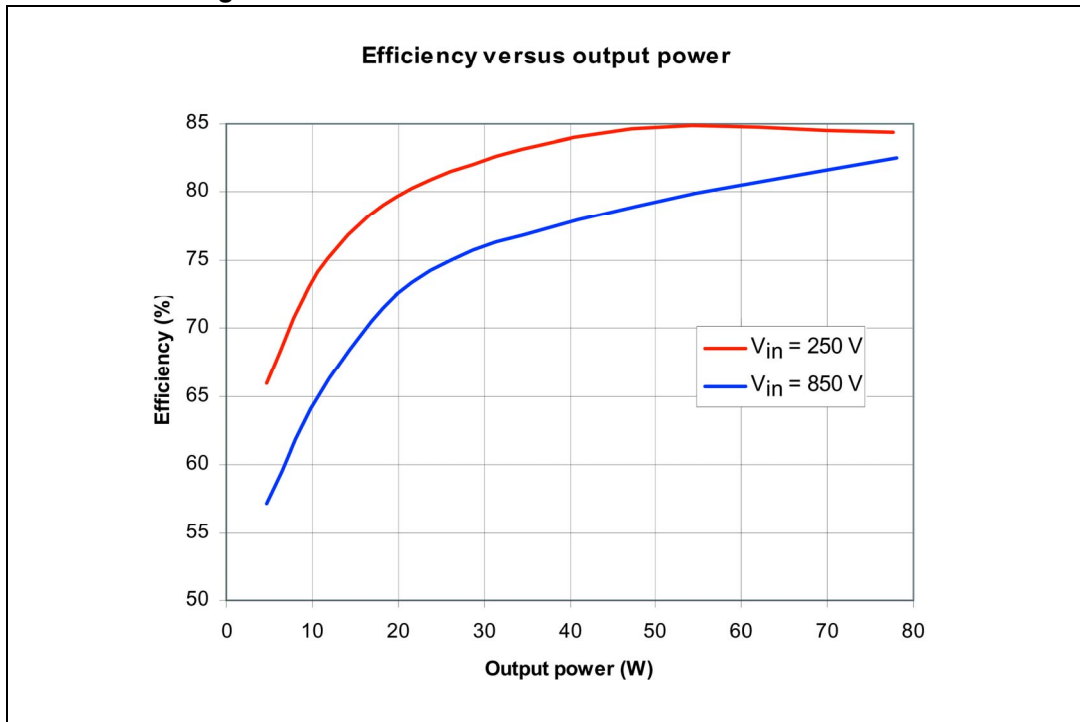


As expected, all requirements have been satisfied by properly choosing the feedback network. Gain bandwidth is quite large, phase margin is around 90° , and system stability margin is improved.

8 Efficiency, waveforms and experimental results

Overall efficiency variation versus output power is illustrated in [Figure 9](#) for two different values of input voltage.

Figure 9. Overall efficiency versus output power for two different values of input voltage



It is worth noting that with low input voltage (red curve), total efficiency is over 80%, and at medium and high load working conditions, reaching almost 85%. Efficiency decreases with input voltage. However, it is above 75% at loads higher than 30% even with maximum input voltage.

Theoretical assumptions made so far have been validated with the use of a demonstration board. A complete description of this board has been carried out and the most meaningful waveforms in any working condition are shown in [Figure 10](#) through [Figure 15](#).

[Figure 10](#), [Figure 11](#) and [Figure 12](#) show the prototype steady state behavior, by indicating the gate voltage (blue waveform), the base current (violet waveform) and the collector voltage (sky blue waveform) at maximum load for different input voltages.

Figure 10. Minimum input voltage-maximum load (250 V - 80 W) in steady state

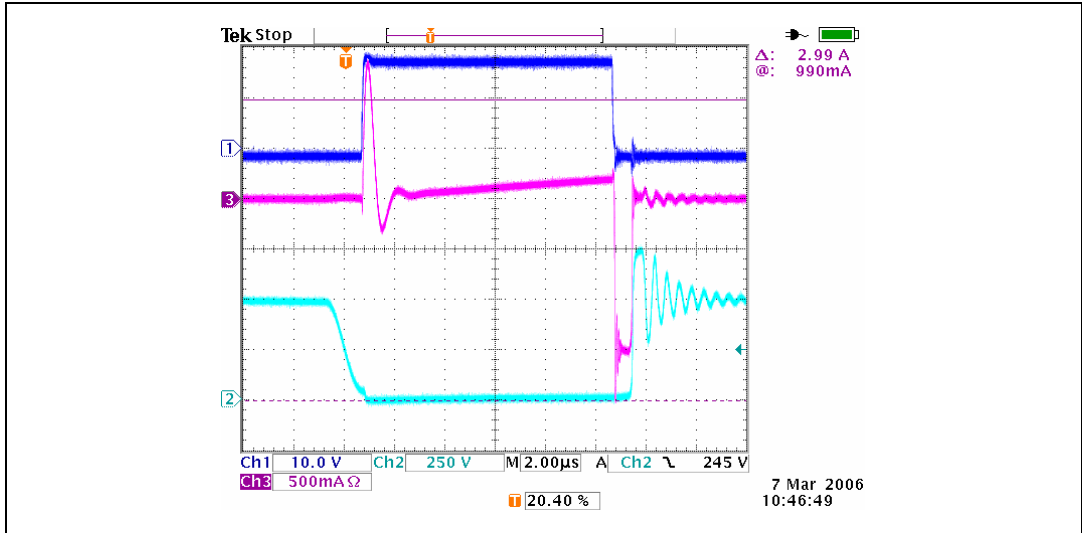


Figure 11. Medium input voltage-maximum load (500 V - 80 W) in steady state

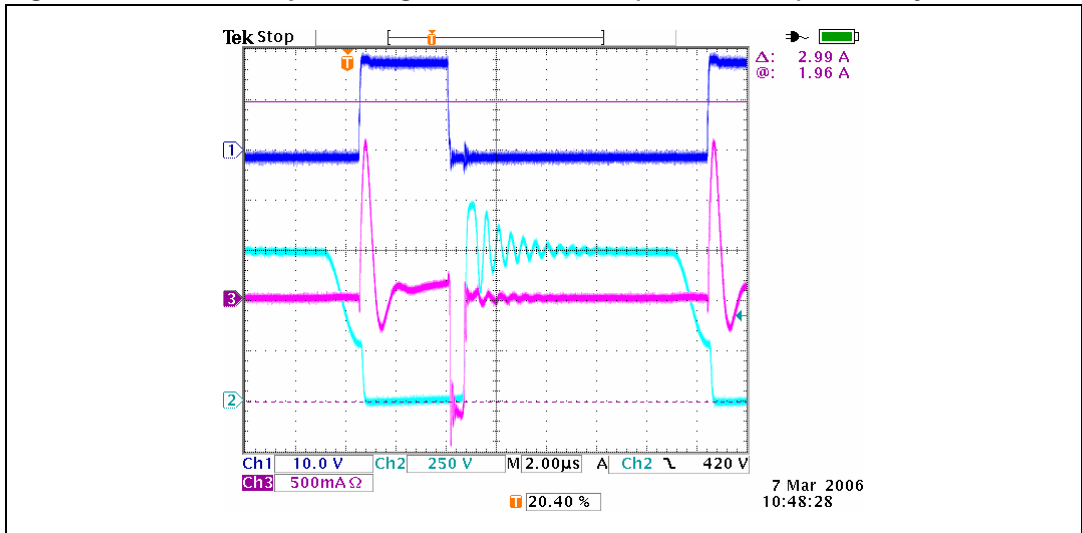
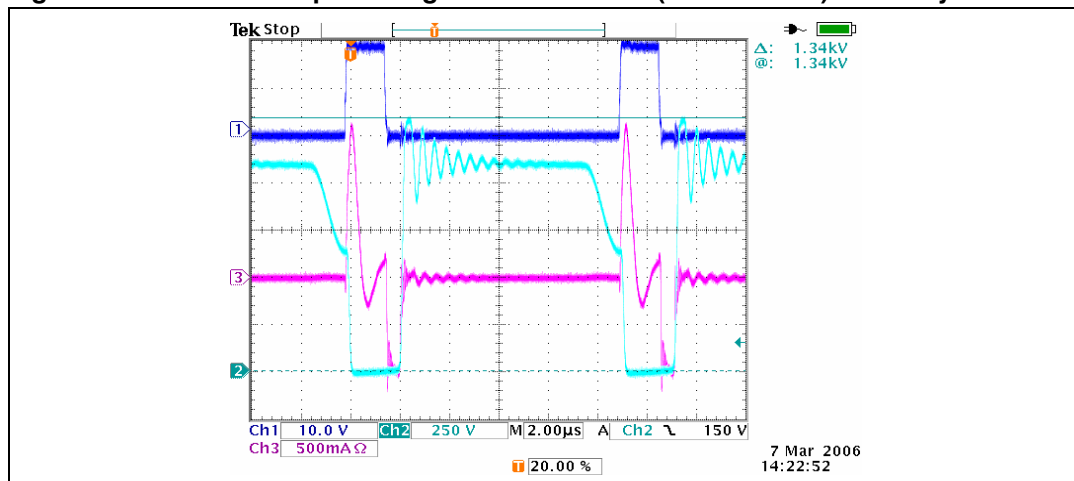


Figure 12. Maximum input voltage-maximum load (850 V - 80 W) in steady state



Waveforms in *Figure 13*, *Figure 14*, and *Figure 15* describe the function of the converter at both low and high load conditions with the same input rectified voltage.

Figure 13. Very low load condition (750 V - 5 W)

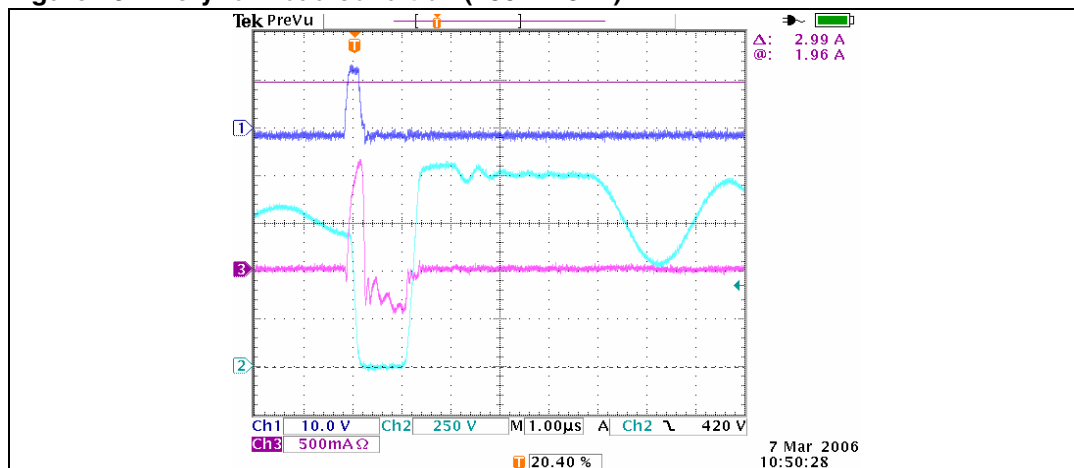


Figure 14. Low load condition (750 V - 24 W)

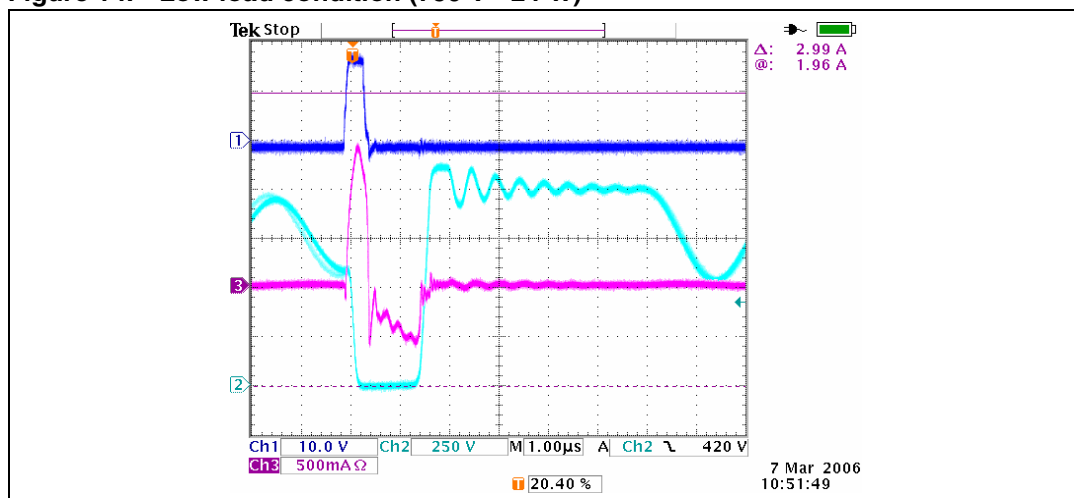
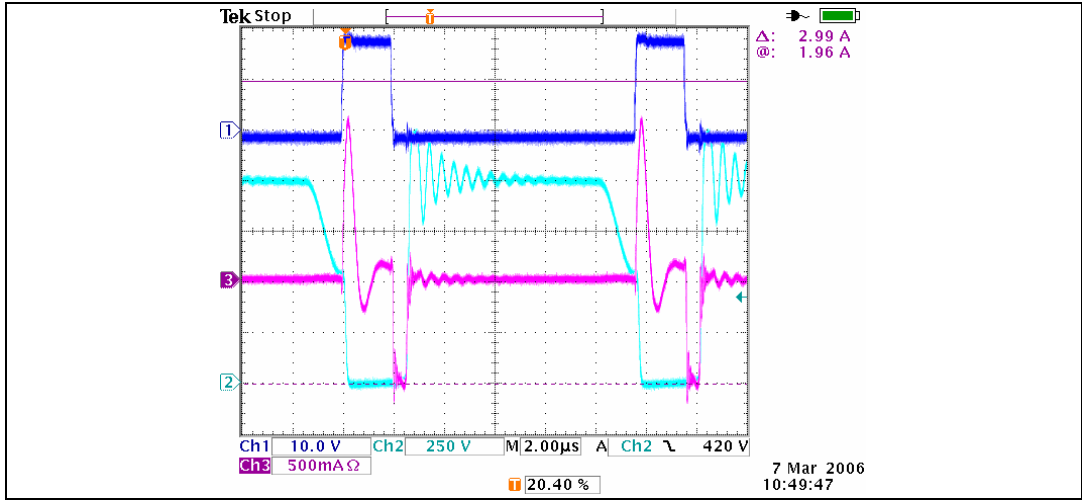
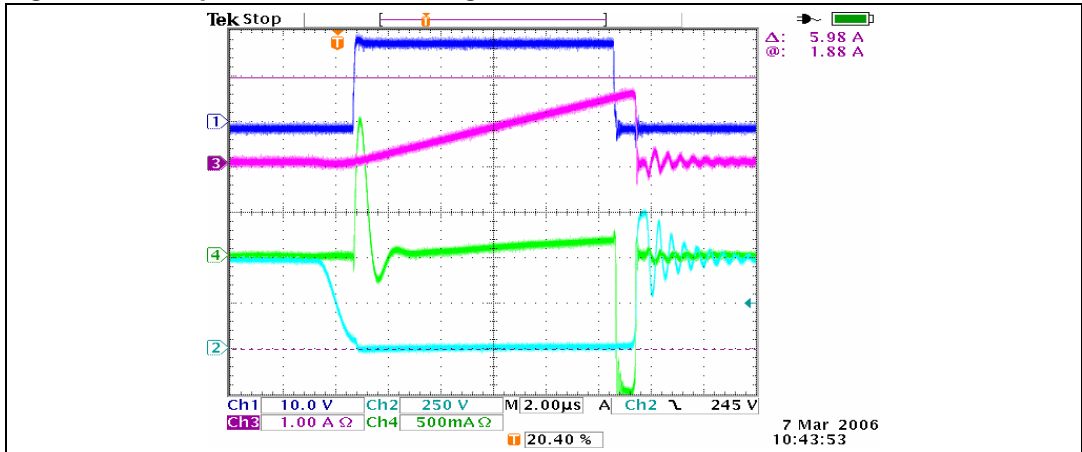


Figure 15. High load condition (750 V - 80 W)



The waveform in [Figure 16](#) illustrates the function of the proportional base driving network. In this graph, collector current is the violet line, while the base current line is light green.

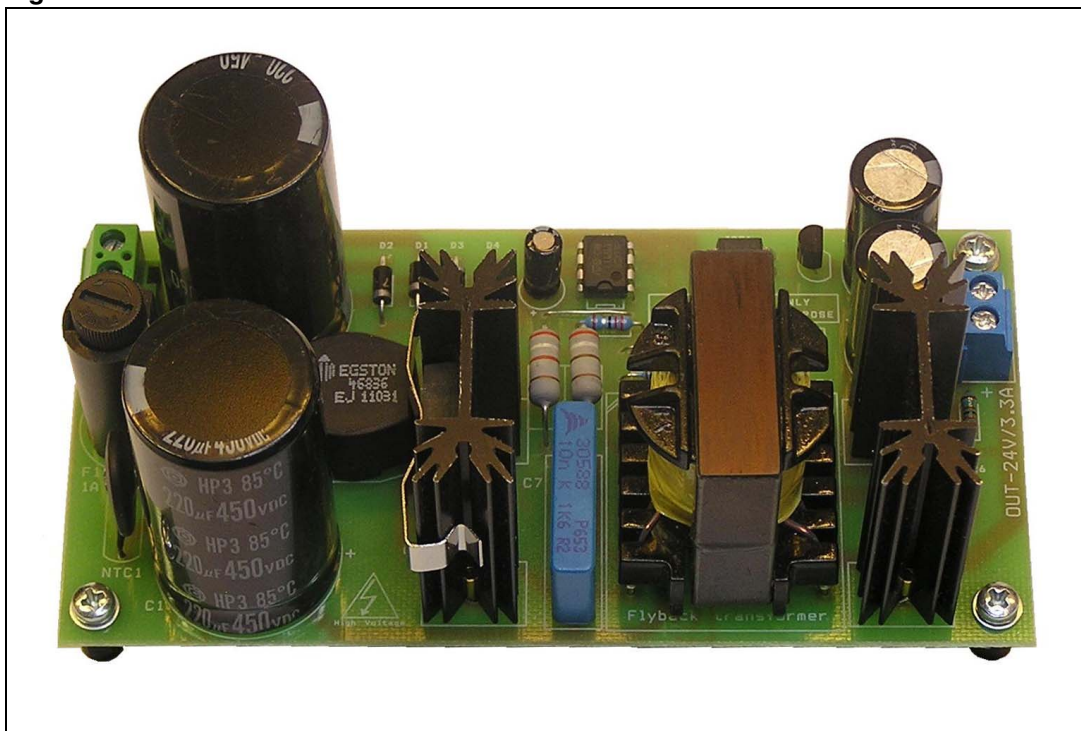
Figure 16. Proportional base driving circuit relevant waveform



9 Board modifications

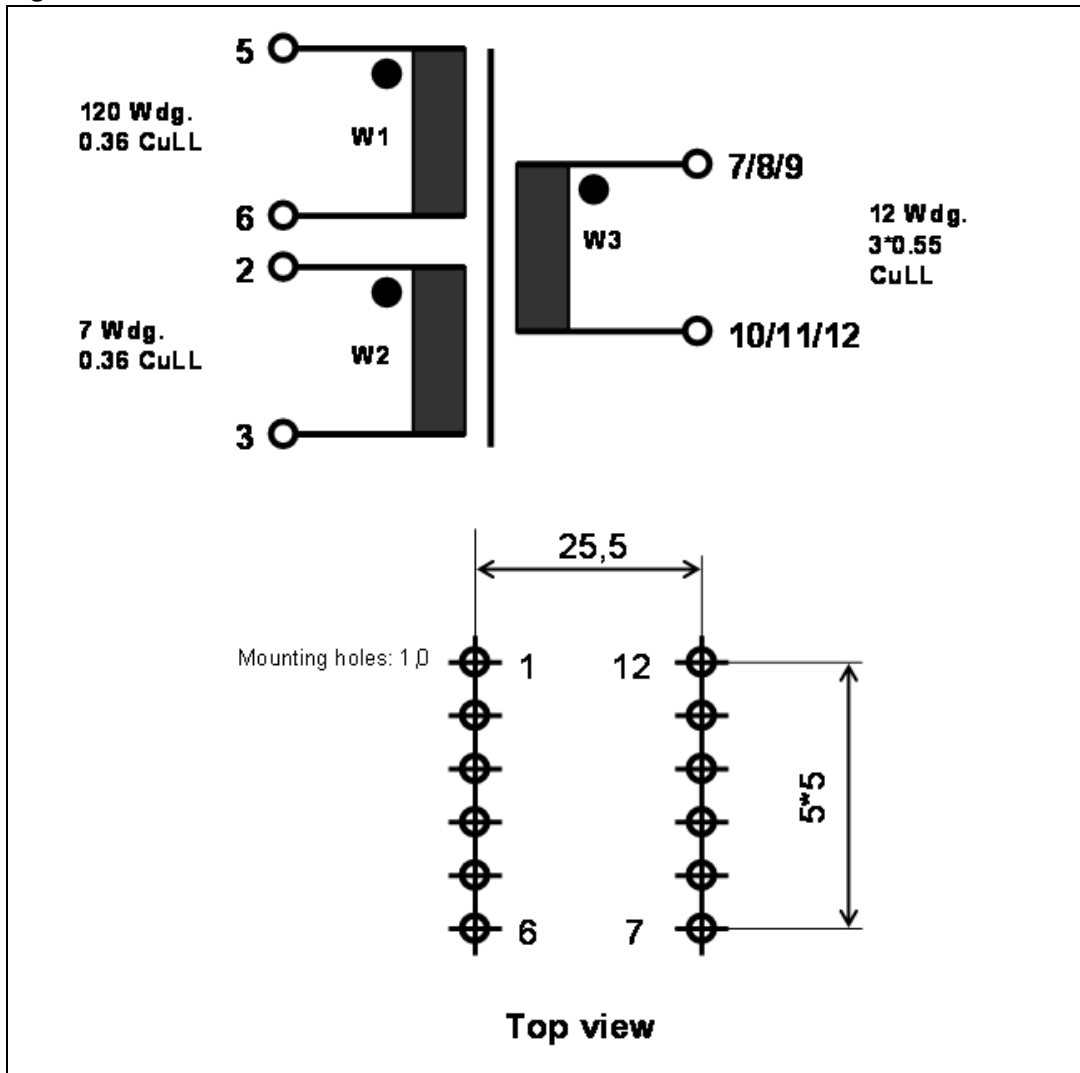
This paragraph has been added following the release of more recent versions of the board STEVAL-ISA019V2 and STEVAL-ISA019V3. For the design procedure and rules, all the preceding paragraphs remain valid. Working conditions have not been changed. The new version was released to take advantage of the size reduction of the SMD components and to insert a new transformer with better coupling between primary inductance and auxiliary winding. The new transformer has been provided in accordance with the application requirements by EGSTON System Electronics Eggenburg GmbH. Moreover, the J2 connector (voltage doubler) has been removed from the board and an NTC resistor 10R (EPCOS B57237S100M) was added in series with the input line to suppress overcurrent peaks during the charge of the bulk capacitor. The complete solution is shown in [Figure 17](#).

Figure 17. STEVAL-ISA019V3



In [Figure 18](#) the complete schematic of the STEVAL-ISA019V3 is provided.

Figure 19. Power transformer EGSTON 45371



The STEVAL-ISA019V2 printed circuit board is shown in [Figure 20](#), [Figure 21](#) and [Figure 22](#).

Figure 20. Silk screen (top side)

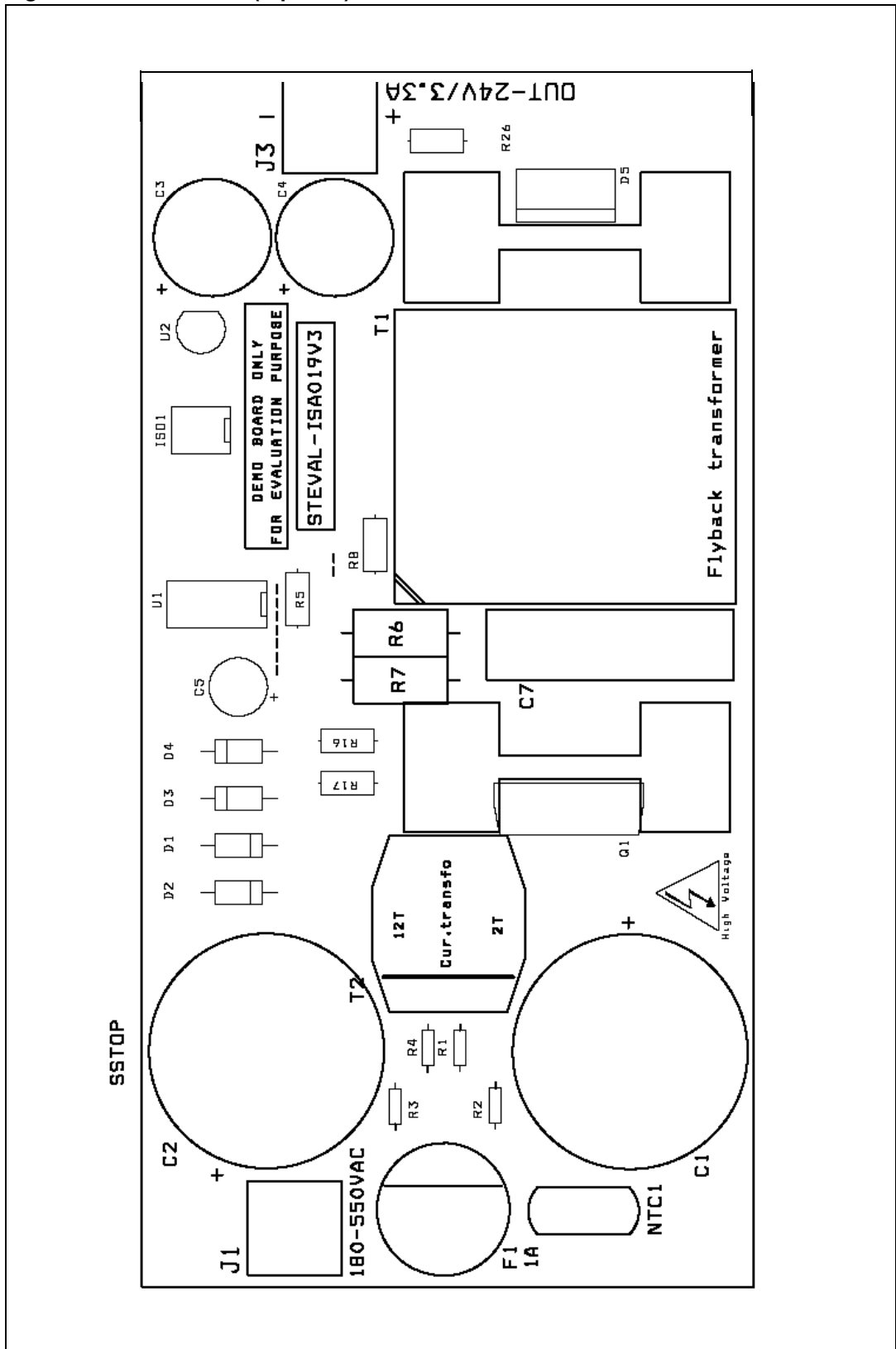


Figure 21. Silk screen (bottom side)

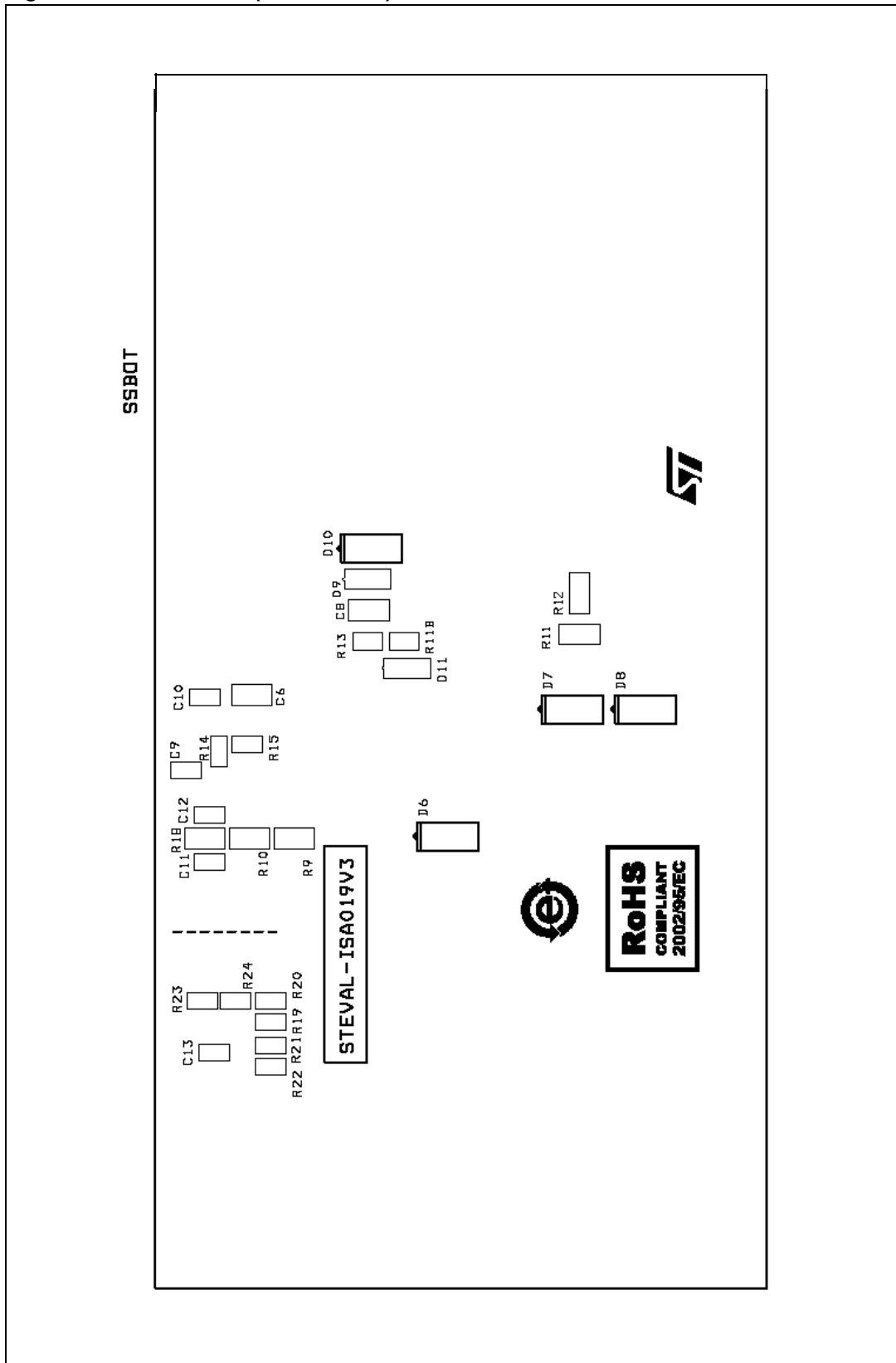


Figure 22. Copper tracks

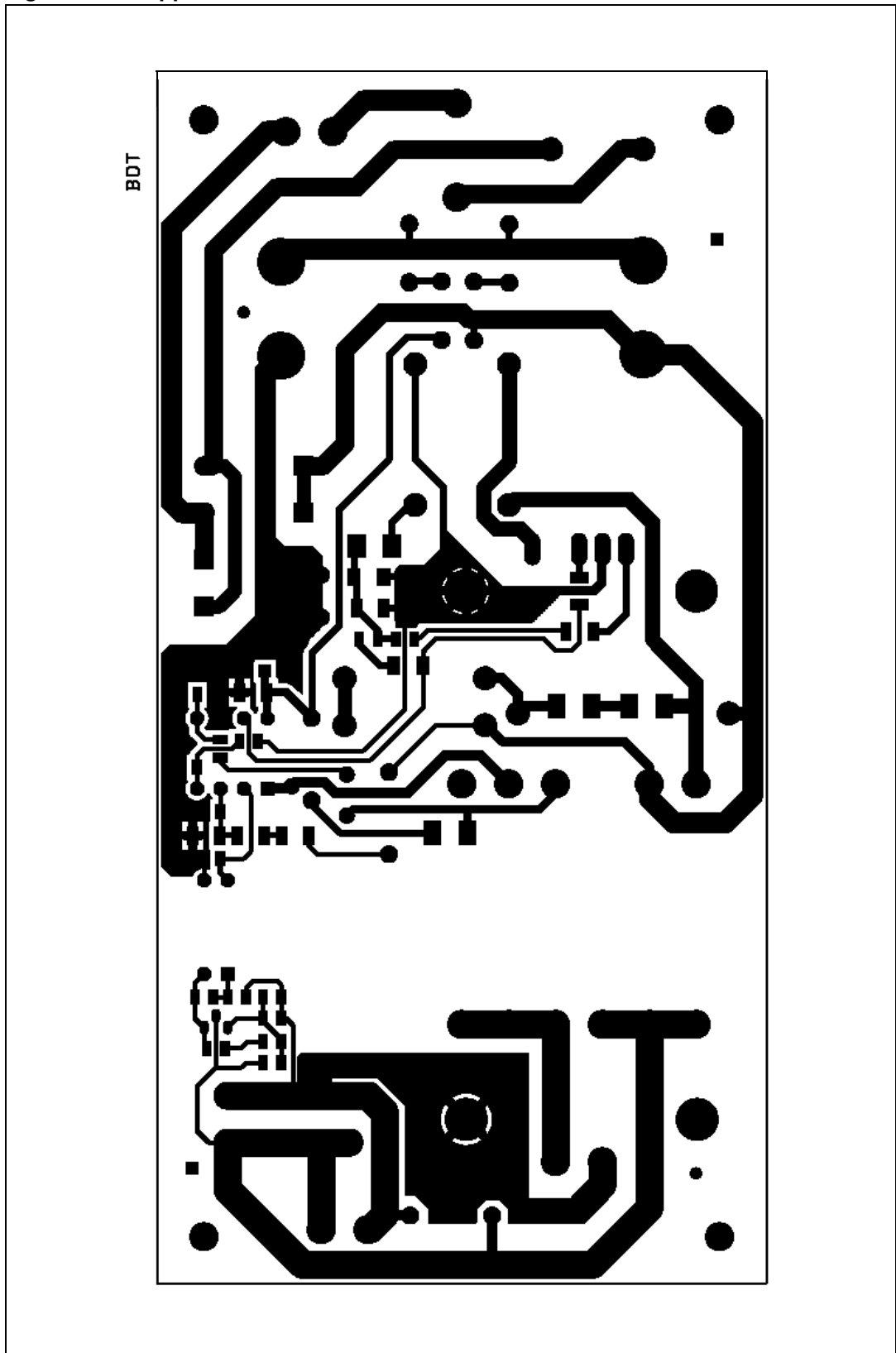


Table 4. Bill of material

Reference	Value / generic part number	Package / class	Manufacturer
C1, C2	220 μ F/450 V	Electrolytic capacitor, 450 V, snap-in, 25*45	EPCOS B43504-A5227-M
C3, C4	1000 μ F/35 V	Electrolytic capacitor, 35 V, 105°C, 12.5*25, low ESR	
C5	47 μ F/35 V	Electrolytic capacitor, 35 V, 105 °C, 5*11	
C6	100 nF	SMD ceramic capacitor CERCAP X7R/50V - 1206	
C12	1 nF	SMD ceramic capacitor CERCAP X7R/50V - 0805	
C9	470 pF	SMD ceramic capacitor CERCAP NPO/50V - 0805	
C10	10 pF	SMD ceramic capacitor CERCAP NPO/50V - 0805	
C11	2.2 nF	SMD ceramic capacitor CERCAP X7R/50V - 0805	
C13	10 nF	SMD ceramic capacitor CERCAP X7R/50V - 0805	
C7	6.8 nF; 1600 VDC	B32653A1682000; polypropylene film pulse capacitor, 1600 VDC, 7.5*16*26.5; 22.5	EPCOS B32653A1682K
C8	150 nF	SMD ceramic capacitor CERCAP X7R/50V - 1206	
D11	LL4148	SMD universal diode	
D9	BZV55C3.0V	Zener diode SMD - SOD80, 3.0 V	
D7, D8, D10	STTH108A	SMD diode, high voltage ultrafast, 800 V, 1 A, SMA	STMicroelectronics
D6	STPS1150A	SMD diode, power Schottky, 150 V, 1 A, SMA	ST
D5	STPS20120D	SMD diode, power Schottky, 120 V, 20 A, TO-220AB	ST
D1, D2, D3, D4	1N4007	HV diode, 1000 V, 1A, DO-41	
F1	T1A	Fuseholder vertical montage, SI-HA#122100	SCHURTER
F1		Fuse 1 A slow, 250 VAC	
het1, het2	8437/38/STB	Heatsink, 8437/38/STB pin 2.2 mm, $R_{thjc} = 11.5 \text{ }^{\circ}\text{C/W}$	
J1	ARK700I/2	Connector ARK700I/2, RM = 5.08 mm	
J3	ARK500/2	Connector ARK500/2, RM = 5 mm	
	KDI6M3X08	Distance column M3, 8 mm	
	clip 00002952	Clip for heatsink 8437	
Q1	STC04IE170HP	4 A, 1700 V ESBT switch, TO-247 4 leads, isolated	ST
R2, R3	200 k Ω	Resistor, size 0204, metal film, 250 V, 0.4 W, 1%	
R12	10 Ω	SMD standard film resistor - 1206 - 1%	
R6, R7	39 k Ω	Resistor, size 0414, metal film, 500 V, 2 W, 5%	
R9, R10	1.1 M Ω	SMD standard film resistor - 1206 - 1%	

Table 4. Bill of material (continued)

Reference	Value / generic part number	Package / class	Manufacturer
R18	10 k Ω	SMD standard film resistor - 1206 - 1%	
R11	1 Ω	SMD standard film resistor - 1206 - 1%	
R11b	0 Ω	SMD standard film resistor - 0805 - 1%	
R13	1 k Ω	SMD standard film resistor - 0805 - 1%	
R14	56 k Ω	SMD standard film resistor - 0805 - 1%	
R15	1 k Ω	SMD standard film resistor - 0805 - 1%	
R16, R17	1.6 Ω	Resistor, size 0207, metal film, 250 V, 0.6 W, 1%	
R24	1.5 k Ω	SMD standard film resistor - 0805 - 1%	
R23	3.3 k Ω	SMD standard film resistor - 0805 - 1%	
R19, R20	47 k Ω	SMD standard film resistor - 0805 - 1%	
R21	15 k Ω	SMD standard film resistor - 0805 - 1%	
R22	2.7 k Ω	SMD standard film resistor - 0805 - 1%	
R5	2.2 Ω	Resistor, size 0207, metal film, 250 V, 0.6 W, 1%	
R8	1.1 M Ω	Resistor, size 0207, metal film, 250 V, 0.6 W, 1%	
R26	1.2 k Ω	Resistor, size 0207, metal film, 250 V, 0.6 W, 5%	
R1, R4	180 k Ω	Resistor, size 0204, metal film, 250 V, 0.4 W, 1%	
T1	45371	EGSTON power transformer	EGSTON 45371
T2	46836	Current transformer, toroid 12.5 mm, 46836	EGSTON 46836
U1	L6565N	STMicroelectronics, PWM SMPS controller, DIP-8	ST
ISO1	PC817B	Optocoupler, SHARP, DIP-4	
U4	TL431AID	Voltage reference, 2.5 V, 1%, TO-92, -40...105 °C	ST
NTC1	10 Ω	NTC resistor 10 Ω ; 16 mm	EPCOS B57237S 100M

10 References

- STMicroelectronics application note AN1889 “ESBT STC03DE170HV in 3-phase auxiliary power supply”
- STMicroelectronics application note AN1262 “OFFLINE FLYBACK CONVERTERS DESIGN METHODOLOGY WITH THE L6590 FAMILY”
- STMicroelectronics application note AN2131 “HIGH POWER 3-PHASE AUXILIARY POWER SUPPLY DESIGN BASED ON L5991 AND ESBT STC08DE150”
- STMicroelectronics L6565 datasheet “QUASI-RESONANT SMPS CONTROLLER”
- STMicroelectronics STC04IE170HV datasheet “Monolithic emitter switched bipolar transistor ESBT[®] 1700 V - 4 A - 0.17 Ω ”
- “Switching Power Supply Design”, McGraw-Hill, Inc.

11 Revision history

Table 5. Document revision history

Date	Revision	Changes
28-Mar-2007	1	First issue
10-Apr-2007	2	<i>Equation 5</i> and <i>Equation 15</i> modified
02-Jul-2007	3	ESBT part number has been updated
20-May-2009	4	<ul style="list-style-type: none"> – <i>Section 9: Board modifications</i> added – Minor text changes throughout the document
19-Apr-2011	5	Document reformatted, updated title, <i>Section 1</i> , <i>Section 3.1.2</i> , <i>Section 3.1.3</i> (modified and added <i>Application specifications</i> and <i>Wires and ferrite used</i>), <i>Section 8</i> , <i>Section 9</i> , (<i>Figure 17</i> to <i>Figure 22</i> , removed <i>Figure 6</i> and <i>8</i> and Section “PCB layout and list of material”, Section “Bill of material” replaced by <i>Table 4</i>), minor text changes and corrected typo throughout the document.

Please Read Carefully:

Information in this document is provided solely in connection with ST products. STMicroelectronics NV and its subsidiaries ("ST") reserve the right to make changes, corrections, modifications or improvements, to this document, and the products and services described herein at any time, without notice.

All ST products are sold pursuant to ST's terms and conditions of sale.

Purchasers are solely responsible for the choice, selection and use of the ST products and services described herein, and ST assumes no liability whatsoever relating to the choice, selection or use of the ST products and services described herein.

No license, express or implied, by estoppel or otherwise, to any intellectual property rights is granted under this document. If any part of this document refers to any third party products or services it shall not be deemed a license grant by ST for the use of such third party products or services, or any intellectual property contained therein or considered as a warranty covering the use in any manner whatsoever of such third party products or services or any intellectual property contained therein.

UNLESS OTHERWISE SET FORTH IN ST'S TERMS AND CONDITIONS OF SALE ST DISCLAIMS ANY EXPRESS OR IMPLIED WARRANTY WITH RESPECT TO THE USE AND/OR SALE OF ST PRODUCTS INCLUDING WITHOUT LIMITATION IMPLIED WARRANTIES OF MERCHANTABILITY, FITNESS FOR A PARTICULAR PURPOSE (AND THEIR EQUIVALENTS UNDER THE LAWS OF ANY JURISDICTION), OR INFRINGEMENT OF ANY PATENT, COPYRIGHT OR OTHER INTELLECTUAL PROPERTY RIGHT.

UNLESS EXPRESSLY APPROVED IN WRITING BY AN AUTHORIZED ST REPRESENTATIVE, ST PRODUCTS ARE NOT RECOMMENDED, AUTHORIZED OR WARRANTED FOR USE IN MILITARY, AIR CRAFT, SPACE, LIFE SAVING, OR LIFE SUSTAINING APPLICATIONS, NOR IN PRODUCTS OR SYSTEMS WHERE FAILURE OR MALFUNCTION MAY RESULT IN PERSONAL INJURY, DEATH, OR SEVERE PROPERTY OR ENVIRONMENTAL DAMAGE. ST PRODUCTS WHICH ARE NOT SPECIFIED AS "AUTOMOTIVE GRADE" MAY ONLY BE USED IN AUTOMOTIVE APPLICATIONS AT USER'S OWN RISK.

Resale of ST products with provisions different from the statements and/or technical features set forth in this document shall immediately void any warranty granted by ST for the ST product or service described herein and shall not create or extend in any manner whatsoever, any liability of ST.

ST and the ST logo are trademarks or registered trademarks of ST in various countries.

Information in this document supersedes and replaces all information previously supplied.

The ST logo is a registered trademark of STMicroelectronics. All other names are the property of their respective owners.

© 2011 STMicroelectronics - All rights reserved

STMicroelectronics group of companies

Australia - Belgium - Brazil - Canada - China - Czech Republic - Finland - France - Germany - Hong Kong - India - Israel - Italy - Japan - Malaysia - Malta - Morocco - Philippines - Singapore - Spain - Sweden - Switzerland - United Kingdom - United States of America

www.st.com